

Study on the electrochemical corrosion and scale growth of ductile iron in water distribution system. PART II

Yimei Tian, Chunlong Liu, Hao Guo^{}, Haiya Zhang, Xingfei Liu, Ying Chen*

Department of Environmental Engineering, School of Environmental Science and Engineering, Tianjin University, Tianjin 300350, China

*E-mail: tjuguohao@163.com

Received: 5 July 2018 / Accepted: 22 August 2018 / Published: 1 October 2018

Long-term contact with carried water makes water supply pipes prone to electrochemical corrosion, which will lead to pipelines leaking or bursting. In this study, a flow corrosion simulation and monitoring system (FCSMS) was designed to systematically study the factors influencing internal corrosion of ductile iron pipes. By using the linear polarization resistance (LPR) method, EIS and the polarization curve test, it was determined how five influencing factors (including temperature and pH) affect the corrosion rate, corrosion scale structure and anodic and cathodic reactions. Then, the effect mechanism of each influencing factor in the internal corrosion process was expounded, and the importance of the influencing factors was determined by correlation analysis: temperature > pH > dissolved oxygen > total hardness > total residual chlorine.

Keywords: water supply pipe, corrosion scale, influencing factors, EIS, polarization curve

1. INTRODUCTION

According to the statistics of the American Water Works Association (AWWA), most of the water supply pipes in the United States are metal pipes, of which grey cast iron pipes account for 38%, ductile iron pipes account for 22%, and steel pipes account for 5%. In China, more than 90% of existing water supply pipes are metal pipes. Compared to other metal pipes, ductile iron pipes have been widely used in water distribution systems (WDSs) due to their high strength and resistance to corrosion. In general, cement mortar linings or other coatings on ductile iron pipes can protect the pipes from corrosion. However, due to technological limitations, accidents during installation and construction, and third-party interference, the integrity of the linings is compromised, and tiny cracks inevitably appear, which will lead to electrochemical corrosion. As corrosion progresses, corrosion

products accumulate at the reaction interface, resulting in expansion forces that cause the coating to fall off. This loss of the coating accelerates the failure of the coating. Therefore, even if a cement mortar lining is adopted in advance, ductile iron pipes still have a large risk of experiencing electrochemical corrosion.

The corrosion of water supply pipelines is affected by various environmental factors, and the mechanism of action of each factor is not yet clear. Simulated pipeline tests based on the weightlessness method [1-4] and electrochemical testing techniques [5-9] are two major corrosion research methods. Based on the above research methods, researchers have conducted extensive research on numerous environmental factors that affect water supply pipeline corrosion, including temperature [10], pH [11], dissolved oxygen [11,12], disinfectants [13-15], and microbes [15-17]. However, neither the weightlessness method nor electrochemical testing technology can simulate the actual flow state of a water supply pipeline. The appearance of rotating disc electrodes (RDEs) and rotating cylinder electrodes (RCEs) [18-22] allows the working electrode to be rotated to simulate a corrosion process under flow conditions. However, the entire test system is still in a sealed circulatory system, and its flow state is very different from that of an actual pipe flow environment. As the reaction progresses, the corrosion product dissolves and falls off into the corrosive medium, causing the corrosive environment to change; thus, test results that deviate from the actual situation may be obtained. Because of these current test conditions, it is difficult to simulate the flow conditions of actual water supply pipes. Therefore, there are few systematic studies on the influencing factors of internal corrosion of ductile iron pipes under actual pipeline flow conditions.

In this study, a flow corrosion simulation and monitoring system (FCSMS) was designed to systematically study the influencing factors on the internal corrosion of ductile iron pipes under actual pipe flow conditions. By using the linear polarization resistance (LPR) method, EIS and the polarization curve test, it was determined how five influencing factors (including temperature and pH) affect the corrosion rate, corrosion scale structure and anodic and cathodic reactions. Then, the effect mechanism of each influencing factor in the internal corrosion process was expounded, and the importance of the influencing factors was determined by correlation analysis.

2. MATERIAL AND METHODS

The flow corrosion simulation and monitoring system (FCSMS) and the working electrode has been described in the companion paper [23].

2.1 Experimental water

To obtain the experimental water, tap water is taken directly from the city's WDS, and the temperature (T) and several water quality indicators including dissolved oxygen (DO), pH, total residual chlorine (TRC) and total hardness (TH) are regulated. Table 1 shows the temperature range and average parameter values of the tap water. Based on this, the horizontal gradient of each influencing factor is set, as shown in Table 2.

Table 1. The temperature range and average parameter values of tap water.

Temperature Range (°C)	DO (mg·L ⁻¹)	pH	TRC (mg·L ⁻¹)	TH (mg·L ⁻¹ as CaCO ₃)
4.9~26.1	6.27	7.13	0.23	237.16

Table 2. Gradient setting of each influencing factor.

Influencing factor	T (°C)	DO (mg·L ⁻¹)	pH	TRC (mg·L ⁻¹)	TH (mg·L ⁻¹ as CaCO ₃)
horizontal gradient	5	1 ^a	6.5	0.1	100
	10	2	7.0	0.3	150
	15	4	7.5	0.5	200
	20	6	8.0	0.7	250
	25	8	8.5	0.9	300

^aThe piping system is difficult to seal completely, and the lowest possible concentration of DO is only 1 mg·L⁻¹.

Based on room temperature, the water temperature is adjusted by an automatic temperature control system in the water-quality renewal system and a heat exchanger in the piping system, and the fluctuation range is ± 1 °C. By adjusting the intake ratio of the O₂/N₂ inflator, the DO concentration of each gradient is obtained, and the fluctuation range is ± 0.5 mg·L⁻¹. The pH is adjusted by dilute nitric acid and sodium hydroxide solutions with a fluctuation range of ± 0.05 . The TRC is adjusted by a dilute sodium hypochlorite solution, and the tap water is exposed for 24 hours before adjustment so that the total residual chlorine content is approximately zero. The fluctuation range is ± 0.5 mg·L⁻¹. To adjust the TH, for a gradient water quality lower than that of the original TH of the tap water, distilled water is used for proportional dilution; for a gradient water quality higher than that of the original TH, dilute calcium nitrate solution (formulated from the reference calcium carbonate solid and dilute nitric acid) is added. The fluctuation range is ± 5 mg·L⁻¹.

2.2 Electrochemical measurement

When the water quality in the piping system is stable, the electrochemical measurement is started. A linear scan is performed every 2 hours to monitor the instantaneous corrosion rate. When the corrosion is in a stable phase, i.e., the variation of the corrosion rate does not exceed 0.1 mm·a⁻¹ for 24 consecutive hours, the EIS measurement is performed first, followed by circulation for half an hour to restore the open-circuit potential of the working electrode to a stable state, and finally, a polarization measurement is conducted. The linear scanning range is ± 15 mV with a rate of 0.5 mV·s⁻¹; the EIS testing range is from 100 kHz to 10 mHz with an amplitude of 10 mV; the polarization measurement scanning range is ± 150 mV; and the rate is 0.5 mV·s⁻¹.

3. RESULTS AND DISCUSSION

3.1 Temperature

3.1.1 Effect on the corrosion rate

Figure 1 shows the variation of the polarization resistance (R_p) at various temperatures. The corrosion process of ductile iron occurs in three stages: Stage I, Stage II, and Stage III. In Stage I, the R_p fluctuates due to the absence of effective protection of the corrosion scale. In Stage II, the corrosion scale grows uniformly, and the R_p increases steadily. In Stage III, since the corrosion scale layer is in a stable state, the R_p also enters a stable state and does not continue to increase over time, which means the corrosion of ductile iron reaches a steady state.

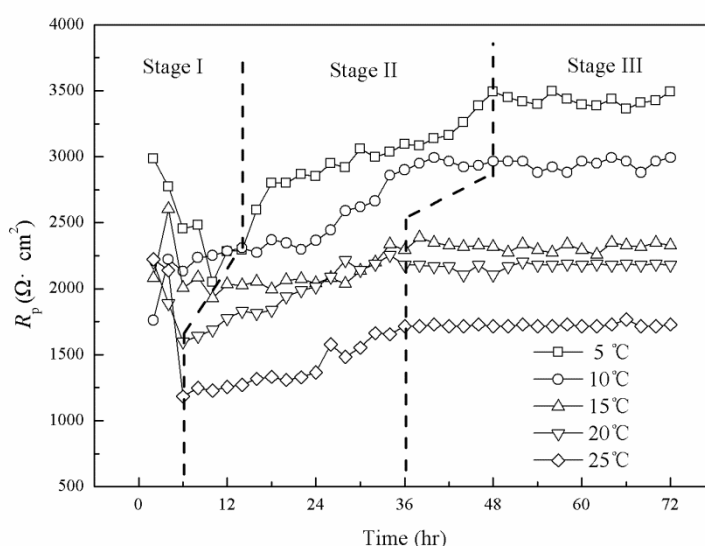


Figure 1. Variation in R_p of ductile iron at various temperatures of 5, 10, 15, 20, 25 °C in tap water. Experimental conditions: DO = 6.0 mg·L⁻¹, pH = 7.0, TRC = 0.20 mg·L⁻¹ and TH = 240 mg·L⁻¹; Electrochemical measurement conditions: scanning range is ±15 mV with a rate of 0.5 mV·s⁻¹.

Table 3. Changing characteristics of each ductile iron corrosion stage at various temperatures of 5, 10, 15, 20, 25 °C in tap water. Experimental conditions: DO = 6.0 mg·L⁻¹, pH = 7.0, TRC = 0.20 mg·L⁻¹ and TH = 240 mg·L⁻¹.

Temperature (°C)	Duration of Stage I (h)	Time length of ductile iron corrosion reaching steady state (h)	R_p of Stage III (Ω·cm ²) ^a
5	18	48	3431.47
10	16	40	2945.42
15	10	38	2312.18
20	6	36	2176.14
25	6	38	1723.75

^aThe average value over 24 hours in Stage III.

Statistics for the duration of each stage and the R_p of Stage III are listed in Table 3. For each temperature, the duration of Stage I ranges from 6 to 18 hours and decreases as the temperature rises. At the same time, the time length of ductile iron corrosion reaching the steady state (Stage III) is shortened as the temperature rises, indicating that increasing the temperature quickly increases the stability of the corrosion scale, which is consistent with existing literature [12].

The corrosion rate, v_{corr} ($\text{mm}\cdot\text{a}^{-1}$), is calculated from the corrosion current density, i_{corr} ($\text{A}\cdot\text{cm}^{-2}$), by equation (1), and the corrosion current density, i_{corr} , is calculated by the Stern-Geary equation (equation 2):

$$v_{corr} = \frac{365 * 24 * 3600 * 10 * i_{corr} * A}{F \rho} \quad (1)$$

$$i_{corr} = \frac{B}{R_p} \quad (2)$$

where i_{corr} is the corrosion current density ($\text{A}\cdot\text{cm}^{-2}$), A is the chemical equivalent of iron ($\text{g}\cdot\text{mol}^{-1}$), F is the Faraday constant ($\text{C}\cdot\text{mol}^{-1}$), ρ is the density of ductile iron ($\text{g}\cdot\text{cm}^{-3}$), B is the Stern B value (mV) and R_p is the polarization resistance ($\Omega\cdot\text{cm}^2$). The Stern B value of Stage III was obtained from a previous experiment and was taken as 20.03 mV.

Figure 2 shows the average corrosion rate for 24 hours in Stage III at various temperatures. The corrosion rate increases with increasing temperature with a clear linear relationship. The analysis shows that increasing the temperature can simultaneously increase the charge transfer rate and the mass transfer rate of the depolarizer, which can increase the corrosion rate overall. This has been proved by several researches [10, 24].

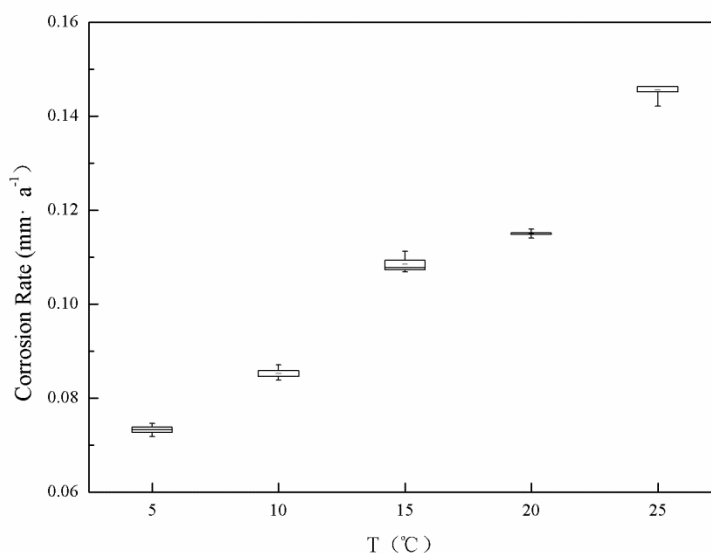


Figure 2. Average corrosion rate of ductile iron in Stage III at various temperatures of 5, 10, 15, 20, 25 °C in tap water. Experimental conditions: DO = 6.0 $\text{mg}\cdot\text{L}^{-1}$, pH = 7.0, TRC = 0.20 $\text{mg}\cdot\text{L}^{-1}$ and TH = 240 $\text{mg}\cdot\text{L}^{-1}$.

3.1.2 Effect on the corrosion scale

EIS measurements were performed to collect electrochemical information about the corrosion scale in Stage III (72 hours) at each temperature, and structural information about the corrosion scale at different temperatures was analysed, as shown in Figure 3. Under low-temperature conditions (5 °C and 10 °C), the impedance spectrum is characterized by double capacitive loops, indicating that the corrosion scale has a double-layer structure. As the temperature increases (above 15 °C), mass diffusion resistance appears, indicating that the corrosion scale in Stage III effectively inhibits further corrosion. Under a low-temperature environment, the growth of the scale is incomplete, and the corrosion is mainly controlled by charge transfer. As the temperature increases, corrosion accelerates, and a complete scale is formed, resulting in a diffusion control phenomenon in Stage III.

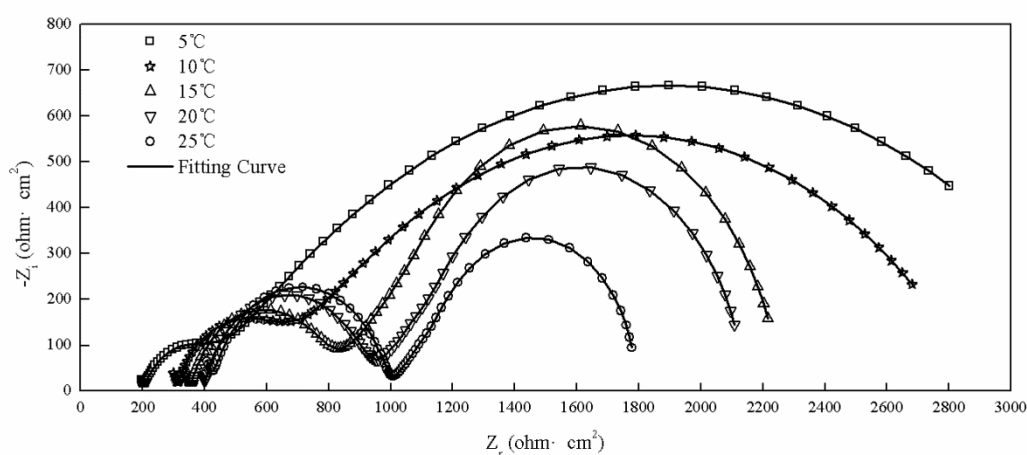


Figure 3. EIS plots of ductile iron in Stage III (72 hours) at various temperatures of 5, 10, 15, 20, 25 °C in tap water. Experimental conditions: DO = 6.0 mg·L⁻¹, pH = 7.0, TRC = 0.20 mg·L⁻¹ and TH = 240 mg·L⁻¹; Electrochemical measurement conditions: EIS testing range is from 100 kHz to 10 mHz with an amplitude of 10 mV. Symbols correspond to various temperatures, and the line corresponds to fitting with the equivalent circuit shown in Figure 4 (b) and (c).

EIS data fitting was performed using the equivalent circuit of Stage II and Stage III of ductile iron corrosion, as shown in Figure 4 (b) and (c), in which R_s represents the solution resistance, Q_f and R_f are the constant phase angle element and equivalent resistance corresponding to the corrosion scale, respectively, Q_{dl} is a constant phase angle element corresponding to a double layer, R_{ct} is the charge transfer resistance and Z_D is the finite diffusion resistance.

The fitting results are shown in Table 4. As the temperature increases, the internal and external corrosion layer resistances (R_i and R_o) continue to increase, while the equivalent capacitances (C_i and C_o) decrease. This result shows that both the internal and external corrosion scales gradually thicken. At the same time, $CPE_{o,n}$ is greater than $CPE_{i,n}$, indicating that the outer corrosion scale is denser than the inner corrosion scale and has better protection. When the temperature is higher than 15 °C, diffusion resistance of the finite layer occurs, and the diffusion coefficient (D_0) and thickness of the diffusion layer (B) both increase with increasing temperature, indicating that a higher temperature is conducive to the growth of the scale.

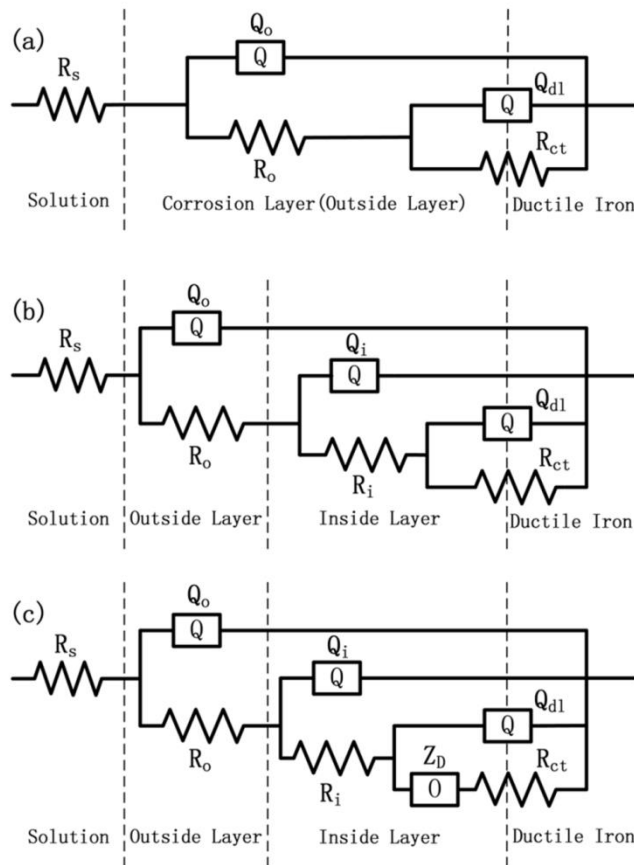


Figure 4. Physical models and equivalent circuits applied to fit the EIS plots of ductile iron.

Table 4. EIS fitting results of ductile iron in Stage III (72 hours) at various temperatures of 5, 10, 15, 20, 25 °C in tap water. Experimental conditions: DO = 6.0 mg·L⁻¹, pH = 7.0, TRC = 0.20 mg·L⁻¹ and TH = 240 mg·L⁻¹.

Electrochemical parameter	Temperature (°C)				
	5	10	15	20	25
C_o ($\mu\text{F}\cdot\text{cm}^{-2}$)	5.374E-04	4.457E-04	2.961E-04	2.185E-04	1.668E-04
$CPE_{o,n}$	0.8217	0.8517	0.8856	0.9003	0.8967
R_o ($\text{ohm}\cdot\text{cm}^2$)	201.4	310.8	348.9	394.0	425.5
C_i ($\mu\text{F}\cdot\text{cm}^{-2}$)	1.484E+00	1.539E+00	1.295E+00	5.929E-01	1.349E-01
$CPE_{i,n}$	0.7836	0.8249	0.8352	0.8502	0.8551
R_i ($\text{ohm}\cdot\text{cm}^2$)	246.0	375.0	428.4	501.6	495.2
C_{dl} ($\mu\text{F}\cdot\text{cm}^{-2}$)	5.148E+02	2.723E+02	3.166E+00	8.720E-01	7.993E-02
$CPE_{dl,n}$	0.5379	0.5830	0.5957	0.5363	0.5063
R_{ct} ($\text{ohm}\cdot\text{cm}^2$)	2926	2218	29.39	29.42	69.74
Y_0 ($\text{S}\cdot\text{sec}^{0.5}\cdot\text{cm}^{-2}$)	—	—	1.262E-03	1.662E-03	2.818E-03
B ($\text{sec}^{0.5}$)	—	—	1.842	2.042	2.258

3.1.3 Effect on the anodic and cathodic reactions

Figure 5 shows the polarization curves of ductile iron in Stage III (72 hours) at various temperatures.

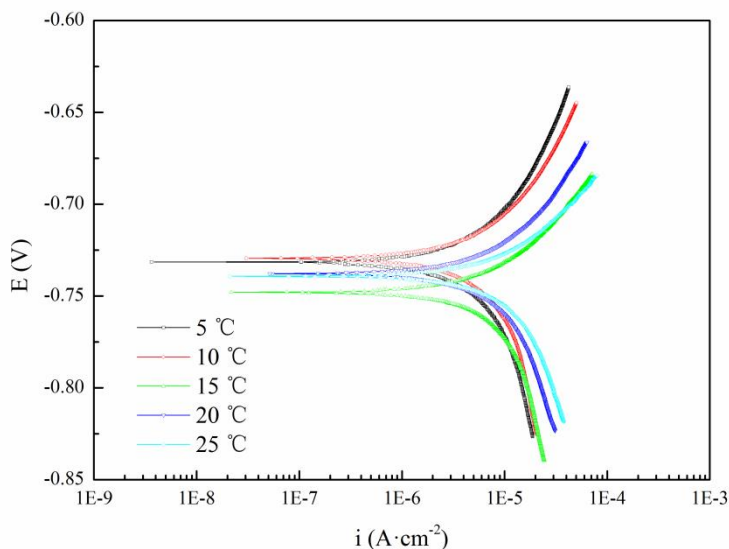


Figure 5. Polarization curves of ductile iron in Stage III (72 hours) at various temperatures of 5, 10, 15, 20, 25 °C in tap water. Experimental conditions: DO = 6.0 mg·L⁻¹, pH = 7.0, TRC = 0.20 mg·L⁻¹ and TH = 240 mg·L⁻¹; Electrochemical measurement conditions: scanning range is ±150 mV with a rate of 0.5 mV·s⁻¹.

Table 5. Fitting results for the polarization curves of ductile iron in Stage III (72 hours) at various temperatures of 5, 10, 15, 20, 25 °C in tap water. Experimental conditions: DO = 6.0 mg·L⁻¹, pH = 7.0, TRC = 0.20 mg·L⁻¹ and TH = 240 mg·L⁻¹.

Temperature (°C)	E_{corr} (V)	b_a (mV)	b_c (mV)
5	-0.731	122.0	204.0
10	-0.730	107.0	241.0
15	-0.748	64.0	232.0
20	-0.738	87.0	168.0
25	-0.739	62.0	150.0

The slopes of the negative and positive polarization curves in the range from ±100 to 125 mV were fit by an artificial fitting method, and the corrosion potential was determined by extrapolation. The fitting results are shown in Table 5. The corrosion potential (E_{corr}) decreases with increasing temperature, indicating that the corrosion tendency of ductile iron is enhanced. Under low-temperature conditions, the Tafel slopes (b_c and b_a) of the cathode and anode are all high, especially the cathodic Tafel slope, indicating that the cathodic and anodic reactions are limited under low-temperature conditions but mainly controlled by the material diffusion of the cathode depolarizer. Under high-temperature conditions, the Tafel slopes of the cathode and anode all show a significant downward

trend, indicating that the increase in temperature can simultaneously promote the development of the cathodic and anodic reactions, which is consistent with existing literature [25].

3.2 DO

3.2.1 Effect on the corrosion rate

Figure 6 shows the variation of R_p at various DO concentrations. The corrosion process of ductile iron also occurs in three stages. At a low DO concentration ($1 \text{ mg}\cdot\text{L}^{-1}$), the R_p rose rapidly in Stage I, and the changes in Stage II and Stage III were small. As the DO concentration increases, the R_p first decreased in Stage I, then increased slowly in Stage II, and finally became stable in Stage III. The reason for this difference is that at low DO concentrations, the depolarizing agent is severely deficient, thus cannot allow the electrochemical reaction to continue. As the DO concentration increases, DO greatly promotes corrosion in Stage I when no stable corrosion scale is formed.

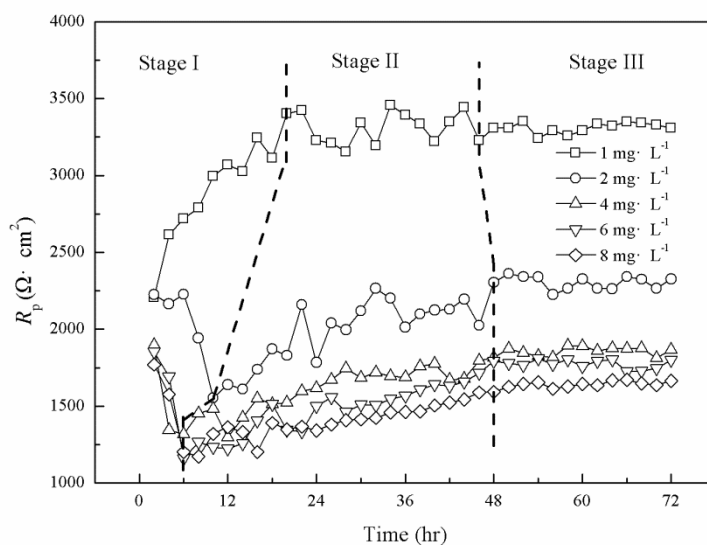


Figure 6. Variation in R_p of ductile iron at various DO concentrations of 1, 2, 4, 6, 8 $\text{mg}\cdot\text{L}^{-1}$ in tap water. Experimental conditions: Temperature = $25 \text{ }^\circ\text{C}$, pH = 7.0, TRC = $0.20 \text{ mg}\cdot\text{L}^{-1}$ and TH = $240 \text{ mg}\cdot\text{L}^{-1}$; Electrochemical measurement conditions: scanning range is $\pm 15 \text{ mV}$ with a rate of $0.5 \text{ mV}\cdot\text{s}^{-1}$.

Statistics for the duration of each stage and the R_p of Stage III are listed in Table 6. The duration of Stage I decreases as the DO concentration increases, and the time length of ductile iron corrosion reaching the steady state (Stage III) is essentially the same, indicating that as the DO concentration increases, the formation of the corrosion scale is significantly accelerated, and the scale is more stable.

Table 6. Changing characteristics of each ductile iron corrosion stage at various DO concentrations of 1, 2, 4, 6, 8 mg·L⁻¹ in tap water. Experimental conditions: Temperature = 25 °C, pH = 7.0, TRC = 0.20 mg·L⁻¹ and TH = 240 mg·L⁻¹.

DO concentration (mg·L ⁻¹)	Duration of Stage I (h)	Time length of ductile iron corrosion reaching steady state (h)	R_p of Stage III ($\Omega \cdot \text{cm}^2$) ^a
1	20	46	3311.00
2	10	48	2304.00
4	6	48	1858.90
6	6	48	1773.40
8	6	48	1644.40

^aThe average value over 24 hours in Stage III.

Figure 7 shows the average corrosion rate for 24 hours in Stage III at various DO concentrations. The corrosion rate increases with increasing DO concentration. When the DO concentration is less than 6 mg·L⁻¹, the rate of increase is large. When the DO concentration is greater than 6 mg L⁻¹, the rate still increases, but the slope decreases. The reason for this finding is that DO, as the main depolarizer, controls the reaction rate of electrochemical corrosion. Furthermore, a high DO concentration is conducive to the stability of the corrosion scale, and the corrosion scale at a high DO concentration is also a factor controlling the corrosion rate.

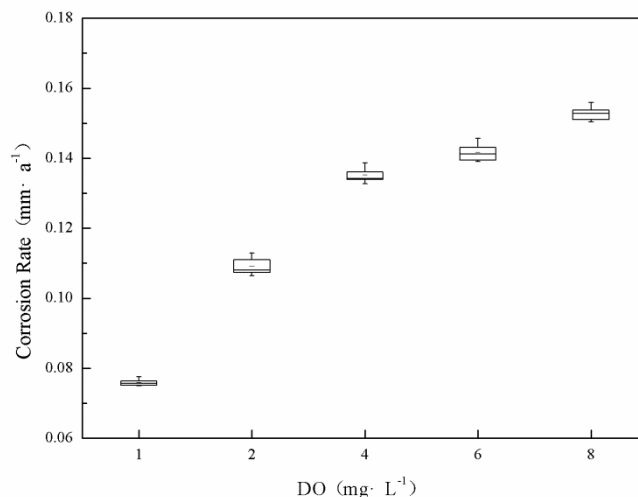


Figure 7. Average corrosion rate of ductile iron in Stage III at various DO concentrations of 1, 2, 4, 6, 8 mg·L⁻¹ in tap water. Experimental conditions: Temperature = 25 °C, pH = 7.0, TRC = 0.20 mg·L⁻¹ and TH = 240 mg·L⁻¹.

3.2.2 Effect on the corrosion scale

Figure 8 shows the EIS plots of Stage III at various DO concentrations. The impedance spectrum at a low DO concentration (1 mg·L⁻¹) has a double-capacitor structure, which is consistent with the characteristics of Stage II. At other DO concentrations, there is a finite diffusion resistance, which is consistent with the impedance characteristics of Stage III.

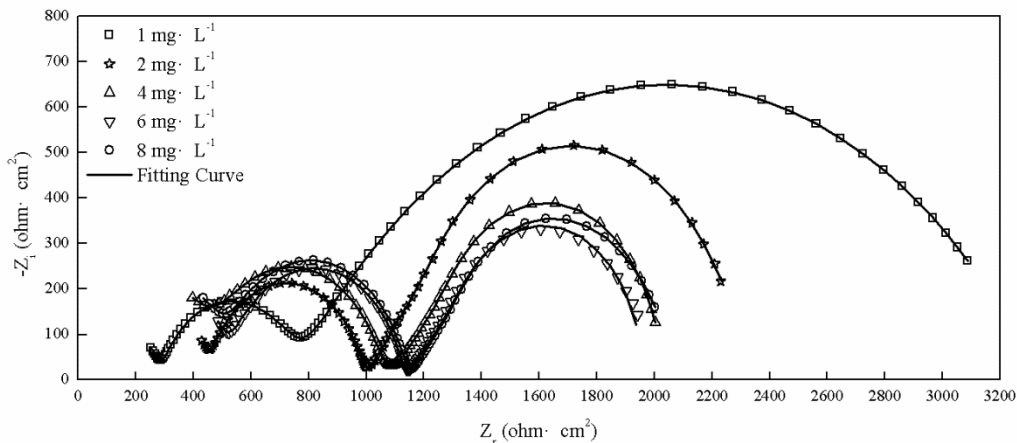


Figure 8. EIS plots of ductile iron in Stage III (72 hours) at various DO concentrations of 1, 2, 4, 6, 8 mg·L⁻¹ in tap water. Experimental conditions: Temperature = 25 °C, pH = 7.0, TRC = 0.20 mg·L⁻¹ and TH = 240 mg·L⁻¹. Electrochemical measurement conditions: EIS testing range is from 100 kHz to 10 mHz with an amplitude of 10 mV. Symbols correspond to various DO concentrations, and the line corresponds to fitting with the equivalent circuit shown in Figure 4 (b) and (c).

EIS data fitting was performed using the equivalent circuit of Stage II and Stage III of the ductile iron corrosion shown in Figure 4 (b) and (c). The fitting results are shown in Table 7. Both the internal and external corrosion scale resistances (R_i and R_o) increased with increasing DO concentration, indicating that DO promoted the growth of the scale layer, which is consistent with existing literature [12]. $CPE_{o,n}$ and $CPE_{i,n}$ continued to increase, indicating that both the internal and external corrosion layers gradually became dense.

Table 7. EIS fitting results of ductile iron in Stage III (72 hours) at various DO concentrations of 1, 2, 4, 6, 8 mg·L⁻¹ in tap water. Experimental conditions: Temperature = 25 °C, pH = 7.0, TRC = 0.20 mg·L⁻¹ and TH = 240 mg·L⁻¹.

Electrochemical parameter	DO concentration (mg·L ⁻¹)				
	1	2	4	6	8
C_o (μF·cm ⁻²)	2.427E-04	1.462E-04	8.462E-04	2.165E-04	4.951E-04
$CPE_{o,n}$	0.8432	0.8609	0.8848	0.8929	0.9080
R_o (ohm·cm ²)	284.9	453.6	495.3	530.3	521.6
C_i (μF·cm ⁻²)	1.291E-01	5.633E-02	4.004E-02	3.759E-02	3.476E-02
$CPE_{i,n}$	0.7836	0.8482	0.8508	0.8496	0.8594
R_i (ohm·cm ²)	475.8	530.5	559.2	598.1	608.1
C_{dl} (μF·cm ⁻²)	2.319E+02	2.262E+01	2.181E+01	1.985E+01	2.063E+01
$CPE_{dl,n}$	0.5949	0.6606	0.7357	0.6026	0.6035
R_{ct} (ohm·cm ²)	2567	11.58	36.68	14.62	20.72
Y_0 (S·sec ^{0.5} ·cm ⁻²)	—	1.614E-03	2.414E-03	2.514E-03	2.505E-03
B (sec ^{0.5})	—	2.145	2.265	2.201	2.315

3.2.3 Effect on the anodic and cathodic reactions

Figure 9 shows the polarization curves of ductile iron in Stage III (72 hours) at various DO concentrations.

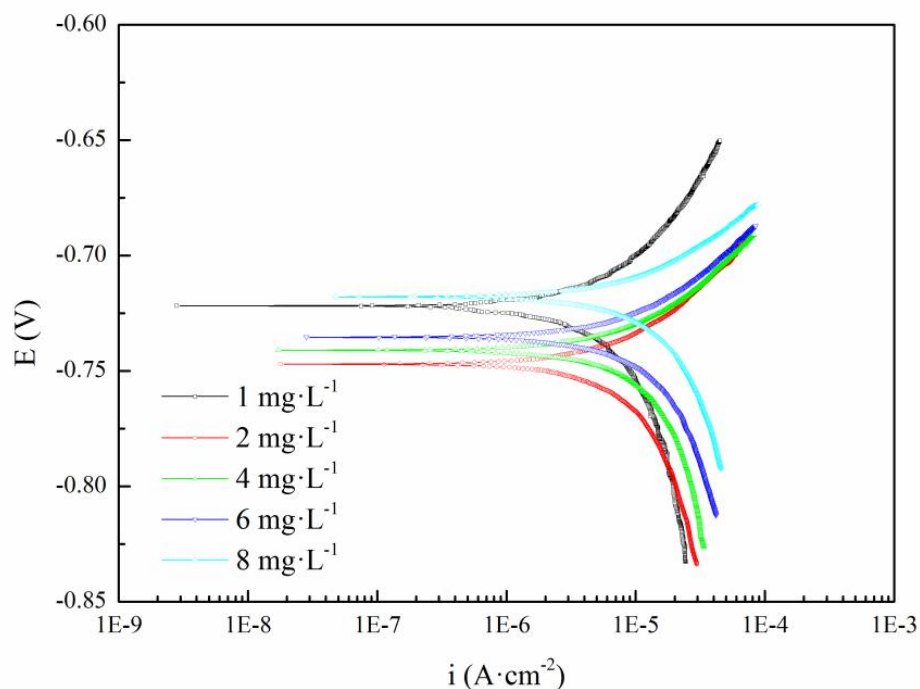


Figure 9. Polarization curves of ductile iron in Stage III (72 hours) at various DO concentrations of 1, 2, 4, 6, 8 $\text{mg}\cdot\text{L}^{-1}$ in tap water. Experimental conditions: Temperature = 25 °C, pH = 7.0, TRC = 0.20 $\text{mg}\cdot\text{L}^{-1}$ and TH = 240 $\text{mg}\cdot\text{L}^{-1}$; Electrochemical measurement conditions: scanning range is ± 15 mV with a rate of 0.5 $\text{mV}\cdot\text{s}^{-1}$.

The slopes of the negative and positive polarization curves in the range of ± 100 to 125 mV were fit by an artificial fitting method, and the corrosion potential was determined by extrapolation. The fitting results are shown in Table 8. As the DO concentration increases, the corrosion potential (E_{corr}) first decreases and then increases, indicating that the corrosion tendency first increases and then decreases. The reason for this finding is that when the DO concentration is very low ($1 \text{ mg}\cdot\text{L}^{-1}$), corrosion does not occur continuously, so the corrosion tendency is extremely weak. Thus, increasing the DO concentration can increase the corrosion tendency rapidly; as the DO concentration continues to increase, the corrosion scale that forms on the surface of ductile iron can effectively reduce the corrosion tendency, which already has been proved by another researcher [12]. As the DO concentration increases, both the cathodic and anodic Tafel slopes (b_c and b_a) show a decreasing trend, but the cathodic Tafel slope decreases more significantly, indicating that DO participates in the corrosion reaction of ductile iron as the main cathode depolarizer. At the same time, as the corrosion product covers the electrode surface, it also plays a role in the anodic reaction.

Table 8. Fitting results for the polarization curves of ductile iron in Stage III (72 hours) at various DO concentrations of 1, 2, 4, 6, 8 mg·L⁻¹ in tap water. Experimental conditions: Temperature = 25 °C, pH = 7.0, TRC = 0.20 mg·L⁻¹ and TH = 240 mg·L⁻¹.

DO concentration (mg·L ⁻¹)	E_{corr} (V)	b_a (mV)	b_c (mV)
1	-0.722	89.2	254.5
2	-0.747	50.1	183.2
4	-0.741	49.4	196.1
6	-0.736	53.4	156.9
8	-0.718	42.6	146.5

3.3 pH

3.3.1 Effect on the corrosion rate

Figure 10 shows the variation of R_p at various pH values. The corrosion process of ductile iron can also be divided into three stages. The higher the pH is, the more obvious the characteristics of three corrosion stages are and the greater the R_p is, indicating that the effect of pH on the corrosion rate is quite obvious and that a low pH has a large effect on the corrosion rate.

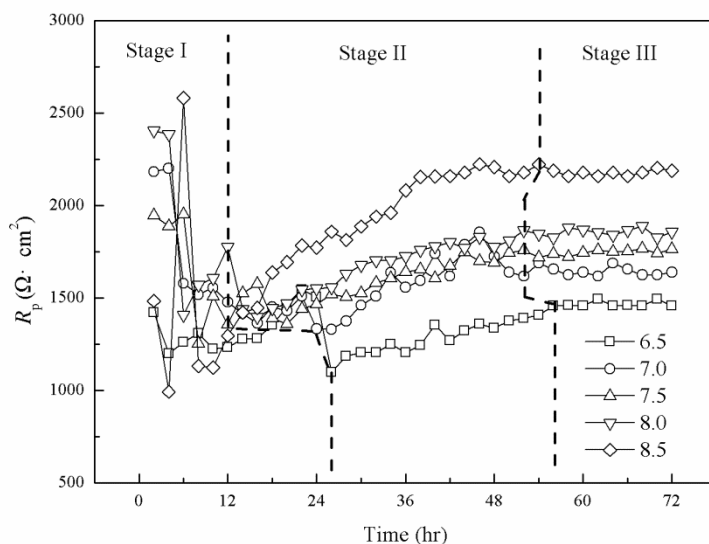


Figure 10. Variation in R_p of ductile iron at various pH values of 6.5, 7.0, 7.5, 8.0, 8.5 in tap water. Experimental conditions: Temperature = 25 °C, DO = 6.0 mg·L⁻¹, TRC = 0.20 mg·L⁻¹ and TH = 240 mg·L⁻¹; Electrochemical measurement conditions: scanning range is ± 15 mV with a rate of 0.5 mV·s⁻¹.

Statistics for the duration of each stage and the R_p of Stage III are listed in Table 9. The lower the pH is, the longer the Stage I is, indicating that the corrosion is more severe at low pH and that the corrosion scale fluctuates more with water quality. For each pH value, the time length of ductile iron corrosion reaching the steady state (Stage III) is essentially the same, but the R_p increases with

increasing pH, and the stability is enhanced, which may be related to the deposition of calcium carbonate at high pH. This result has already been proved by several researches [26-29].

Table 9. Changing characteristics of each ductile iron corrosion stage at various pH values of 6.5, 7.0, 7.5, 8.0, 8.5 in tap water. Experimental conditions: Temperature = 25 °C, DO = 6.0 mg·L⁻¹, TRC = 0.20 mg·L⁻¹ and TH = 240 mg·L⁻¹.

pH	Duration of Stage I (h)	Time length of ductile iron corrosion reaching steady state (h)	R_p of Stage III ($\Omega \cdot \text{cm}^2$) ^a
6.5	26	56	1447.27
7.0	24	50	1642.92
7.5	20	50	1746.70
8.0	16	52	1852.07
8.5	12	38	2179.19

^aThe average value over 24 hours in Stage III.

Figure 11 shows the average corrosion rate for 24 hours in Stage III at various pH values. The corrosion rate decreases linearly with increasing pH. The reason for this finding is that at low pH, there are many hydrogen ions in the water that can directly participate in the corrosion process to absorb electrons, so the corrosion changes from oxygen-absorption corrosion to hydrogen evolution corrosion. At high pH, the deposition of calcium carbonate causes a significant increase in the stability of the scale layer, and the corrosion rate decreases linearly.

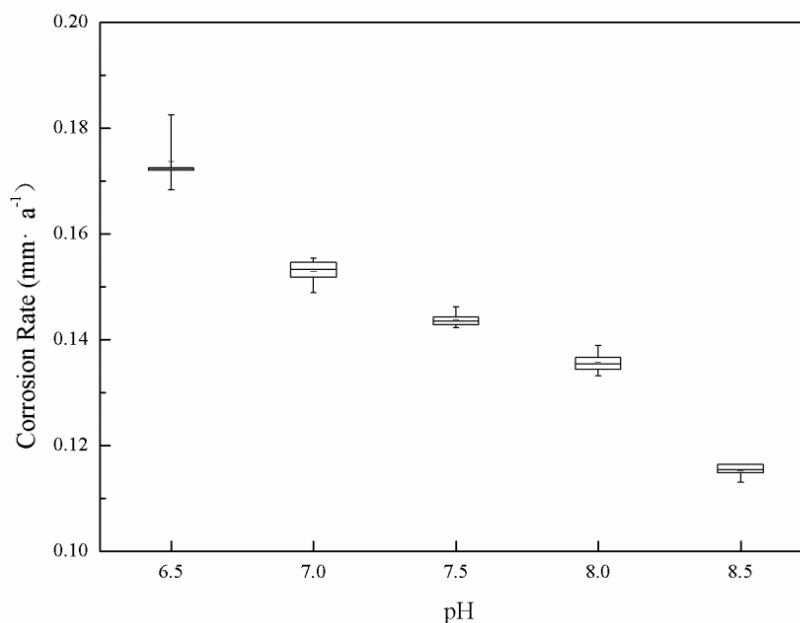


Figure 11. Average corrosion rate of ductile iron in Stage III at various pH values of 6.5, 7.0, 7.5, 8.0, 8.5 in tap water. Experimental conditions: Temperature = 25 °C, DO = 6.0 mg·L⁻¹, TRC = 0.20 mg·L⁻¹ and TH = 240 mg·L⁻¹.

3.3.2 Effect on the corrosion scale

Figure 12 shows the EIS plots of Stage III at various pH values. Different from the plots for temperature and DO, the EIS plots at different pH values show the characteristics of the impedance spectrum of the stable scale layer; i.e., there is finite layer diffusion impedance at low frequencies. This shows that a denser corrosion scale is formed at different pH values, and the corrosion process is diffusion controlled.

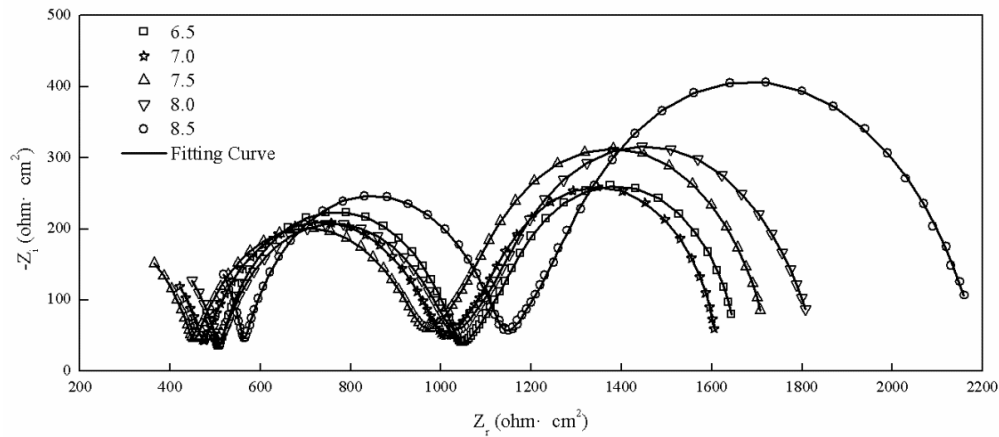


Figure 12. EIS plots of ductile iron in Stage III (72 hours) at various pH values of 6.5, 7.0, 7.5, 8.0, 8.5 in tap water. Experimental conditions: Temperature = 25 °C, DO = 6.0 mg·L⁻¹, TRC = 0.20 mg·L⁻¹ and TH = 240 mg·L⁻¹; Electrochemical measurement conditions: EIS testing range is from 100 kHz to 10 mHz with an amplitude of 10 mV. Symbols correspond to various pH values, and the line corresponds to fitting with the equivalent circuit shown in Figure 4 (c).

Table 10. EIS fitting results of ductile iron in Stage III (72 hours) at various pH values of 6.5, 7.0, 7.5, 8.0, 8.5 in tap water. Experimental conditions: Temperature = 25 °C, DO = 6.0 mg·L⁻¹, TRC = 0.20 mg·L⁻¹ and TH = 240 mg·L⁻¹.

Electrochemical parameter	pH				
	6.5	7.0	7.5	8.0	8.5
C_o ($\mu\text{F}\cdot\text{cm}^{-2}$)	4.240E-04	7.893E-04	1.323E-03	7.411E-04	5.403E-04
$CPE_{o,n}$	0.9103	0.8965	0.9089	0.8876	0.9533
R_o ($\text{ohm}\cdot\text{cm}^2$)	508.4	475.4	453.1	509.5	551.3
C_i ($\mu\text{F}\cdot\text{cm}^{-2}$)	6.715E-01	8.175E-01	1.106E+00	8.444E-01	4.705E-01
$CPE_{i,n}$	0.8965	0.8616	0.8536	0.8676	0.9071
R_i ($\text{ohm}\cdot\text{cm}^2$)	521.9	510.4	496.3	500.6	564.6
C_{dl} ($\mu\text{F}\cdot\text{cm}^{-2}$)	7.449E+01	2.150E+01	2.744E+01	1.479E+01	1.376E+02
$CPE_{dl,n}$	0.7836	0.7609	0.6977	0.639	0.7379
R_{ct} ($\text{ohm}\cdot\text{cm}^2$)	6.948	8.793	6.057	5.497	47.95
Y_0 ($\text{S}\cdot\text{sec}^{0.5}\cdot\text{cm}^{-2}$)	3.350E-03	3.049E-03	2.252E-03	1.852E-03	1.218E-03
B ($\text{sec}^{0.5}$)	2.094	1.893	1.756	1.540	1.248

EIS data fitting was performed using the equivalent circuit of Stage III of the ductile iron corrosion shown in Figure 4 (c). The fitting results are shown in Table 10. With an increase in pH, both the internal and external corrosion scale resistances (R_i and R_o) first decrease and then increase, meaning that the protection of the scale first decreases and then increases. Comparing $CPE_{o,n}$ and $CPE_{i,n}$, the outer scale is denser, and when the pH is 8.5, the density is significantly higher than that at other pH values, which indicates that the density of the corrosion scale is significantly enhanced at high pH. This is mainly because calcium carbonate in an alkaline environment is more easily deposited, i.e., mainly covering the outer surface of the scale and partially embedded in the inner layer, and thus, the protective property of the corrosion scale is significantly improved. At low pH, the corrosion rate is high, and more corrosion products are formed, so the density and thickness of the scale at low pH are higher than those at neutral pH.

3.3.3 Effect on the anodic and cathodic reactions

Figure 13 shows the polarization curves of ductile iron in Stage III (72 hours) at various pH values.

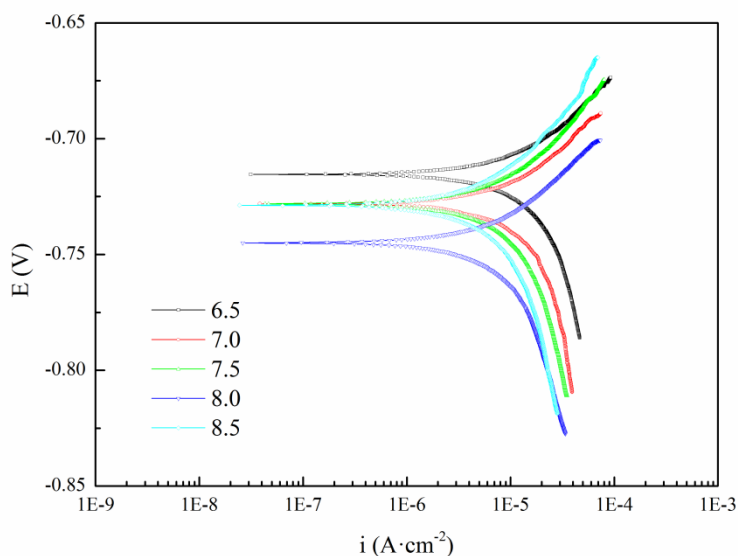


Figure 13. Polarization curves of ductile iron in Stage III (72 hours) at various pH values of 6.5, 7.0, 7.5, 8.0, 8.5 in tap water. Experimental conditions: Temperature = 25 °C, DO = 6.0 mg·L⁻¹, TRC = 0.20 mg·L⁻¹ and TH = 240 mg·L⁻¹; Electrochemical measurement conditions: scanning range is ±15 mV with a rate of 0.5 mV·s⁻¹.

The slope of the negative and positive polarization curves in the range of ±100 to 125 mV were fit by an artificial fitting method, and the corrosion potential was determined by extrapolation. The fitting results are shown in Table 11. As the pH increased, the corrosion potential (E_{corr}) showed an upward trend, indicating that the corrosion tendency was weakened. Both the cathodic and anodic Tafel slopes (b_c and b_a) fluctuated and increased, and the diffusion control characteristics of the

cathodic polarization curve were significantly enhanced, indicating that a pH increase suppressed both the anodic and cathodic reactions but mainly suppressed the cathodic reaction.

Table 11. Fitting results for the polarization curves of ductile iron in Stage III (72 hours) at various pH values of 6.5, 7.0, 7.5, 8.0, 8.5 in tap water. Experimental conditions: Temperature = 25 °C, DO = 6.0 mg·L⁻¹, TRC = 0.20 mg·L⁻¹ and TH = 240 mg·L⁻¹.

pH	E_{corr} (V)	b_a (mV)	b_c (mV)
6.5	-0.716	47.0	154.0
7.0	-0.728	37.0	184.0
7.5	-0.728	55.0	172.0
8.0	-0.745	43.0	155.0
8.5	-0.749	83.0	205.0

3.4 TRC

3.4.1 Effect on the corrosion rate

Figure 14 shows the variation of R_p at various TRC concentrations. The corrosion process of ductile iron also occurs in three stages. At different TRC concentrations, the three stages of corrosion can be clearly distinguished. However, there is no obvious linear relationship between the R_p and the TRC concentration in Stage III, indicating that TRC is not directly involved in the electrochemical reaction process of ductile iron.

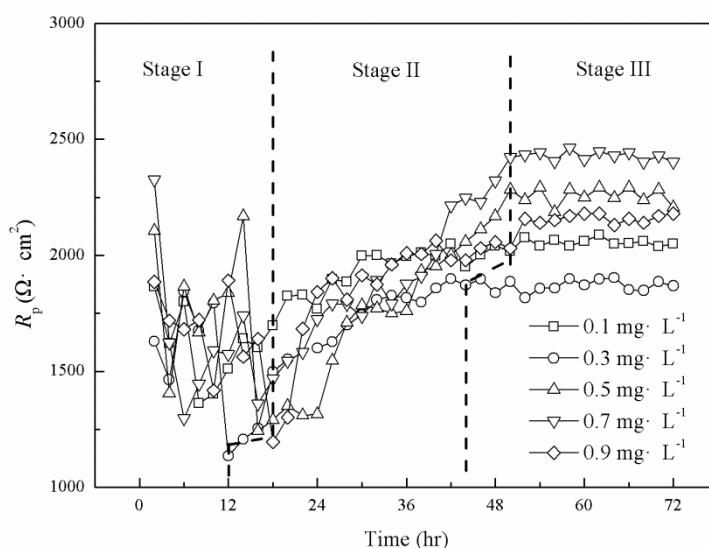


Figure 14. Variation in R_p of ductile iron at various TRC concentrations of 0.1, 0.3, 0.5, 0.7, 0.9 mg·L⁻¹ in tap water. Experimental conditions: Temperature = 25 °C, DO = 6.0 mg·L⁻¹, pH = 7.0 and TH = 240 mg·L⁻¹; Electrochemical measurement conditions: scanning range is ± 15 mV with a rate of 0.5 mV·s⁻¹.

Statistics for the duration of each stage and the R_p of Stage III are listed in Table 12. The duration of Stage I increases with the increase of TRC concentration, and the time length of ductile

iron corrosion reaching the steady state (Stage III) is also the same, indicating that TRC has a certain influence on the stability of the scale and that a high concentration of TRC is not conducive to the stability of the scale.

Table 12. Changing characteristics of each ductile iron corrosion stage at various TRC concentrations of 0.1, 0.3, 0.5, 0.7, 0.9 mg·L⁻¹ in tap water. Experimental conditions: Temperature = 25 °C, DO = 6.0 mg·L⁻¹, pH = 7.0 and TH = 240 mg·L⁻¹.

TRC concentration (mg·L ⁻¹)	Duration of Stage I (h)	Time length of ductile iron corrosion reaching steady state (h)	R _p of Stage III (Ω·cm ²) ^a
0.1	12	50	2053.30
0.3	18	44	1870.51
0.5	18	50	2257.65
0.7	18	50	2427.81
0.9	18	50	2148.64

^aThe average value over 24 hours in Stage III.

Figure 15 shows the average corrosion rate for 24 hours in Stage III at various TRC concentrations. The corrosion rate fluctuates with the TRC concentration, but the overall change is not dramatic and is essentially stable at 0.1200 mm·a⁻¹. Compared with other factors, the TRC concentration has little effect on the corrosion rate. In addition to the influence of the TRC concentration on the corrosion process, the chloride ions do not directly participate in the corrosion electrochemical reaction but have a destructive effect on the scale, resulting in the instability of the scale. However, due to continuous corrosion, the damaged scale will be repaired by newly formed corrosion products. Therefore, TRC has some influence on the corrosion process, but the overall effect is not great.

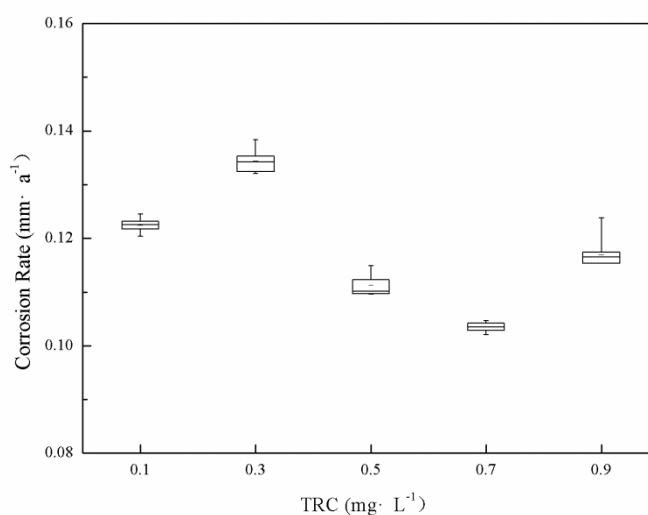


Figure 15. Average corrosion rate of ductile iron in Stage III at various TRC concentrations of 0.1, 0.3, 0.5, 0.7, 0.9 mg·L⁻¹ in tap water. Experimental conditions: Temperature = 25 °C, DO = 6.0 mg·L⁻¹, pH = 7.0 and TH = 240 mg·L⁻¹.

3.4.2 Effect on the corrosion scale

Figure 16 shows the EIS plots of Stage III at various TRC concentrations. Consistent with the characteristics of the EIS plot at various pH values, the middle and high frequencies form two capacitive reactance arcs, and the low frequency is the finite diffusion layer impedance.

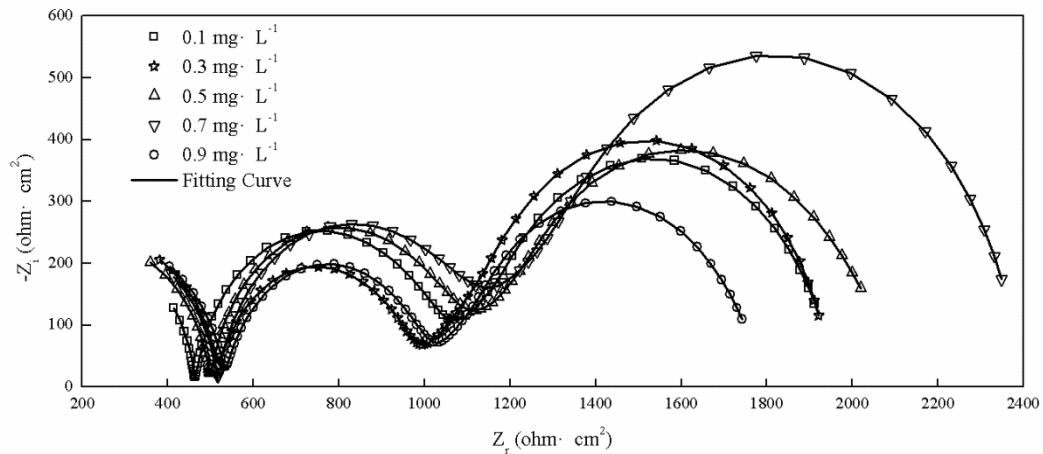


Figure 16. EIS plots of ductile iron in Stage III (72 hours) at various TRC concentrations of 0.1, 0.3, 0.5, 0.7, 0.9 mg·L⁻¹ in tap water. Experimental conditions: Temperature = 25 °C, DO = 6.0 mg·L⁻¹, pH = 7.0 and TH = 240 mg·L⁻¹; Electrochemical measurement conditions: EIS testing range is from 100 kHz to 10 mHz with an amplitude of 10 mV. Symbols correspond to various TRC concentrations, and the line corresponds to fitting with the equivalent circuit shown in Figure 4 (c).

Table 13. EIS fitting results of ductile iron in Stage III (72 hours) at various TRC concentrations of 0.1, 0.3, 0.5, 0.7, 0.9 mg·L⁻¹ in tap water. Experimental conditions: Temperature = 25 °C, DO = 6.0 mg·L⁻¹, pH = 7.0 and TH = 240 mg·L⁻¹.

Electrochemical parameter	TRC concentration (mg·L ⁻¹)				
	0.1	0.3	0.5	0.7	0.9
C_o ($\mu\text{F}\cdot\text{cm}^{-2}$)	9.723E-04	1.640E-03	1.736E-03	1.261E-03	1.352E-03
$CPE_{o,n}$	0.956	0.9471	0.9388	0.9298	0.9088
R_o ($\text{ohm}\cdot\text{cm}^2$)	460.2	508.4	495.5	511.4	534.9
C_i ($\mu\text{F}\cdot\text{cm}^{-2}$)	5.563E+00	1.575E+00	6.490E+00	8.560E+00	2.792E+00
$CPE_{i,n}$	0.9115	0.8918	0.9177	0.9042	0.8878
R_i ($\text{ohm}\cdot\text{cm}^2$)	560.6	447.3	563.2	584.6	461.7
C_{dl} ($\mu\text{F}\cdot\text{cm}^{-2}$)	1.808E+01	3.540E+00	2.208E+00	5.302E+00	1.297E+00
$CPE_{dl,n}$	6.46E-01	6.51E-01	5.38E-01	7.18E-01	5.57E-01
R_{ct} ($\text{ohm}\cdot\text{cm}^2$)	9.924	4.149	4.538	1.035	1.303
Y_0 ($\text{S}\cdot\text{sec}^{0.5}\cdot\text{cm}^{-2}$)	2.210E-03	2.060E-03	1.860E-03	1.670E-03	2.400E-03
B ($\text{sec}^{0.5}$)	2.060	2.027	1.966	2.156	1.930

EIS data fitting was performed using the equivalent circuit of Stage III of the ductile iron corrosion shown in Figure 4 (c). The fitting results are shown in Table 13. With the increase in the

TRC concentration, both the internal and external corrosion scale resistances (R_i and R_o) fluctuate, but the overall difference is not significant, indicating that TRC has no decisive effect on scale growth. The n values of the internal and external corrosion scales decrease, indicating that the density of the corrosion scale is decreased, which is related to the destructive effect of the chloride ions in the TRC on the scale.

3.4.3 Effect on the anodic and cathodic reactions

Figure 17 shows the polarization curves of ductile iron in Stage III (72 hours) at various TRC concentrations.

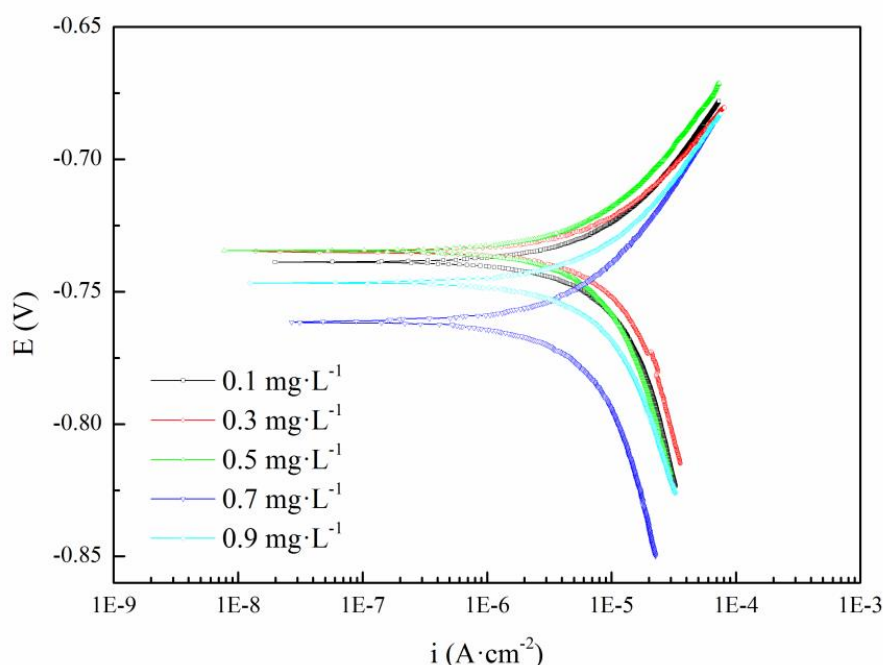


Figure 17. Polarization curves of ductile iron in Stage III (72 hours) at various TRC concentrations of 0.1, 0.3, 0.5, 0.7, 0.9 $\text{mg}\cdot\text{L}^{-1}$ in tap water. Experimental conditions: Temperature = 25 °C, DO = 6.0 $\text{mg}\cdot\text{L}^{-1}$, pH = 7.0 and TH = 240 $\text{mg}\cdot\text{L}^{-1}$; Electrochemical measurement conditions: scanning range is ± 15 mV with a rate of 0.5 $\text{mV}\cdot\text{s}^{-1}$.

The slope of the negative and positive polarization curves in the range of ± 100 to 125 mV were fit by an artificial fitting method, and the corrosion potential was determined by extrapolation. The fitting results are shown in Table 14. With the increase in the TRC concentration, the oxidizability of TRC can make the surface scale dense, leading to an increase in the corrosion potential (E_{corr}). When a certain concentration (0.7 $\text{mg}\cdot\text{L}^{-1}$) is reached, the chlorine ions generated by the decomposition and reduction of hypochlorous acid have a destructive effect on the surface scale, resulting in a decrease in the corrosion potential. The anodic Tafel slope (b_a) remains essentially unchanged, indicating that TRC has no effect on the anodic reaction; the cathodic Tafel slope (b_c) decreases, indicating that the increase in the TRC concentration promotes the cathodic reaction.

Table 14. Fitting results for the polarization curves of ductile iron in Stage III (72 hours) at various TRC concentrations of 0.1, 0.3, 0.5, 0.7, 0.9 mg·L⁻¹ in tap water. Experimental conditions: Temperature = 25 °C, DO = 6.0 mg·L⁻¹, pH = 7.0 and TH = 240 mg·L⁻¹.

TRC concentration (mg·L ⁻¹)	E_{corr} (V)	b_a (mV)	b_c (mV)
0.1	-0.739	66.0	170.0
0.3	-0.735	57.0	188.0
0.5	-0.735	62.0	155.0
0.7	-0.762	73.0	158.0
0.9	-0.747	67.0	136.0

3.5 TH

3.5.1 Effect on the corrosion rate

Figure 18 shows the variation of R_p at various TH concentrations. The corrosion process of ductile iron also occurs in three stages. At different TH concentrations, the R_p changes are essentially the same. The R_p of Stage III increases slightly with increasing TH concentration, which means that increasing TH is beneficial to the stability of the scale to some extent.

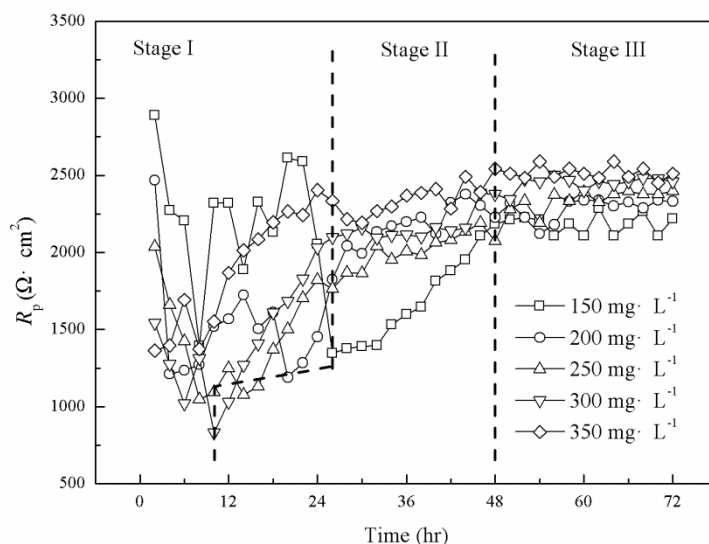


Figure 18. Variation in R_p of ductile iron at various TH concentrations of 150, 200, 250, 300, 350 mg·L⁻¹ in tap water. Experimental conditions: Temperature = 25 °C, DO = 6.0 mg·L⁻¹, pH = 7.0 and TRC = 0.20 mg·L⁻¹; Electrochemical measurement conditions: scanning range is ± 15 mV with a rate of 0.5 mV·s⁻¹.

Statistics for the duration of each stage and the R_p of Stage III are listed in Table 15. As the TH concentration increases, the duration of Stage I decreases, and the R_p of Stage III increases, indicating that the higher the TH concentration is, the more stable the corrosion scale becomes. This is consistent with existing literature [13, 30] and the presence of CaCO₃ makes the scales become a protective film.

Table 15. Changing characteristics of each ductile iron corrosion stage at various TH concentrations of 150, 200, 250, 300, 350 mg·L⁻¹ in tap water. Experimental conditions: Temperature = 25 °C, DO = 6.0 mg·L⁻¹, pH = 7.0 and TRC = 0.20 mg·L⁻¹.

TH concentration (mg·L ⁻¹)	Duration of Stage I (h)	Time length of ductile iron corrosion reaching steady state (h)	R _p of Stage III (Ω·cm ²) ^a
150	26	46	2287.04
200	18	48	2345.78
250	10	48	2452.39
300	10	46	2516.61
350	10	50	2556.10

^aThe average value over 24 hours in Stage III.

Figure 19 shows the average corrosion rate for 24 hours in Stage III at various TH concentrations. The corrosion rate shows a slight downward trend with increasing TH concentration. High TH concentrations increase the deposition of calcium carbonate. The scale can provide better protection in the case of a consistent corrosion environment.

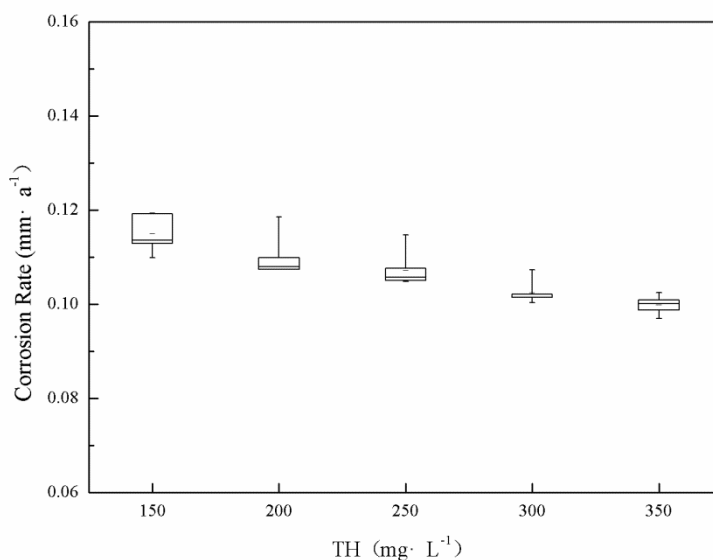


Figure 19. Average corrosion rate of ductile iron in Stage III at various TH concentrations of 150, 200, 250, 300, 350 mg·L⁻¹ in tap water. Experimental conditions: Temperature = 25 °C, DO = 6.0 mg·L⁻¹, pH = 7.0 and TRC = 0.20 mg·L⁻¹.

3.5.2 Effect on the corrosion scale

Figure 20 shows the EIS plots of Stage III at various TH concentrations. Consistent with the characteristics of the EIS plot at various pH values and TRC concentrations, the middle- and high-frequency regions have two capacitive reactance arcs, and the low-frequency region is the finite diffusion layer impedance.

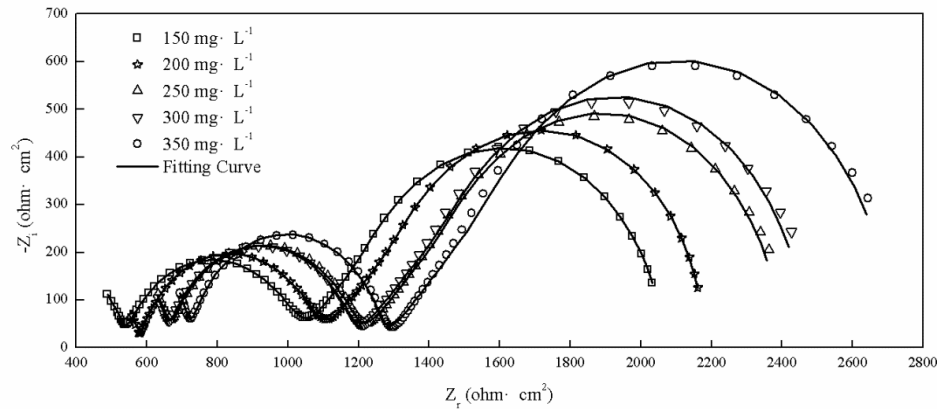


Figure 20. EIS plots of ductile iron in Stage III (72 hours) at various TH concentrations of 150, 200, 250, 300, 350 $\text{mg}\cdot\text{L}^{-1}$ in tap water. Experimental conditions: Temperature = 25 °C, DO = 6.0 $\text{mg}\cdot\text{L}^{-1}$, pH = 7.0 and TRC = 0.20 $\text{mg}\cdot\text{L}^{-1}$; Electrochemical measurement conditions: EIS testing range is from 100 kHz to 10 mHz with an amplitude of 10 mV. Symbols correspond to various TH concentrations, and the line corresponds to fitting with the equivalent circuit shown in Figure 4 (c).

EIS data fitting was performed using the equivalent circuit of Stage III of the ductile iron corrosion shown in Figure 4 (c). The fitting results are shown in Table 16. As the TH concentration increases, both the internal and external corrosion scale resistances (R_i and R_o) increase, and the equivalent capacitances of the internal and external corrosion scales (C_i and C_o) decrease, indicating that TH is conducive to the stability of the scale. At the same time, R_o is always greater than R_i , and C_o is always smaller than C_i , indicating that the stability of the external corrosion scale is significantly higher than that of the internal corrosion scale. It can be assumed that TH mainly acts on the internal corrosion scale.

Table 16. EIS fitting results of ductile iron in Stage III (72 hours) at various TH concentrations of 150, 200, 250, 300, 350 $\text{mg}\cdot\text{L}^{-1}$ in tap water. Experimental conditions: Temperature = 25 °C, DO = 6.0 $\text{mg}\cdot\text{L}^{-1}$, pH = 7.0 and TRC = 0.20 $\text{mg}\cdot\text{L}^{-1}$.

Electrochemical parameter	TH concentration ($\text{mg}\cdot\text{L}^{-1}$)				
	150	200	250	300	350
C_o ($\mu\text{F}\cdot\text{cm}^{-2}$)	5.048E-04	3.869E-04	3.175E-04	2.953E-04	2.751E-04
$CPE_{o,n}$	0.8512	0.8604	0.9011	0.9139	0.9300
R_o ($\text{ohm}\cdot\text{cm}^2$)	540.4	579.1	660.3	659.1	723.2
C_i ($\mu\text{F}\cdot\text{cm}^{-2}$)	7.452E-01	4.607E-01	3.318E-01	3.131E-01	2.676E-01
$CPE_{i,n}$	0.8103	0.8208	0.8529	0.8568	0.8889
R_i ($\text{ohm}\cdot\text{cm}^2$)	478.5	491.6	522.9	521.2	555.8
C_{dl} ($\mu\text{F}\cdot\text{cm}^{-2}$)	5.475E+00	4.261E+00	8.205E+00	8.983E+00	2.419E+01
$CPE_{dl,n}$	0.6323	0.5713	0.5984	0.5986	0.6954
R_{ct} ($\text{ohm}\cdot\text{cm}^2$)	12.32	16.59	17.24	12.83	3.886
Y_0 ($\text{S}\cdot\text{sec}^{0.5}\cdot\text{cm}^{-2}$)	2.025E-03	1.984E-03	1.833E-03	1.732E-03	1.700E-03
B ($\text{sec}^{0.5}$)	2.115	2.171	2.297	2.348	2.556

3.5.3 Effect on the anodic and cathodic reactions

Figure 21 shows the polarization curves of ductile iron in Stage III (72 hours) at various TRC concentrations.

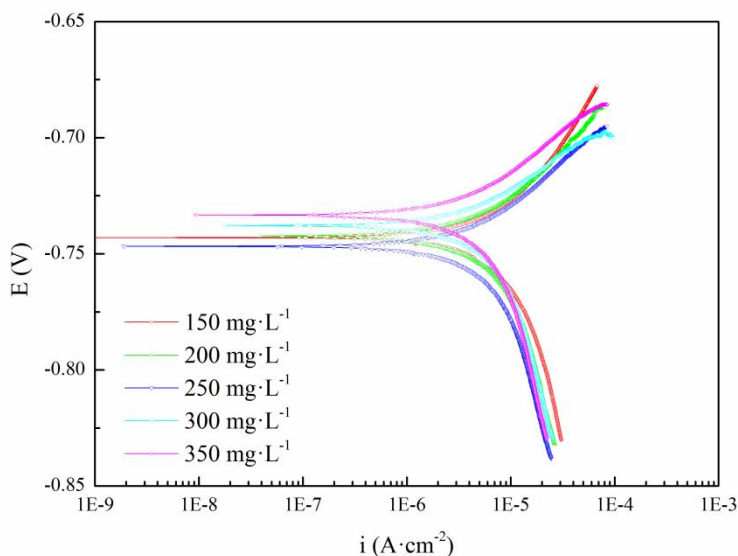


Figure 21. Polarization curves of ductile iron in Stage III (72 hours) at various TH concentrations of 150, 200, 250, 300, 350 $\text{mg}\cdot\text{L}^{-1}$ in tap water. Experimental conditions: Temperature = 25 °C, DO = 6.0 $\text{mg}\cdot\text{L}^{-1}$, pH = 7.0 and TRC = 0.20 $\text{mg}\cdot\text{L}^{-1}$; Electrochemical measurement conditions: scanning range is ± 15 mV with a rate of $0.5 \text{ mV}\cdot\text{s}^{-1}$.

Table 17. Fitting results for the polarization curves of ductile iron in Stage III (72 hours) at various TH concentrations of 150, 200, 250, 300, 350 $\text{mg}\cdot\text{L}^{-1}$ in tap water. Experimental conditions: Temperature = 25 °C, DO = 6.0 $\text{mg}\cdot\text{L}^{-1}$, pH = 7.0 and TRC = 0.20 $\text{mg}\cdot\text{L}^{-1}$.

TH concentration ($\text{mg}\cdot\text{L}^{-1}$)	E_{corr} (V)	b_a (mV)	b_c (mV)
150	-0.743	74.0	162.0
200	-0.742	54.0	181.0
250	-0.747	36.0	178.0
300	-0.738	14.0	171.0
350	-0.733	27.0	198.0

The slope of the negative and positive polarization curves in the range of ± 100 to 125 mV were fit by an artificial fitting method, and the corrosion potential was determined by extrapolation. The fitting results are shown in Table 17. As the TH concentration increases, the corrosion potential (E_{corr}) first decreases and then increases. The reason for this finding is that no calcium carbonate protective film is formed when the TH concentration is low, and as the TH concentration increases, the conductivity of tap water increases, resulting in an increased corrosion tendency. When the TH concentration exceeds 300 $\text{mg}\cdot\text{L}^{-1}$, the protective film formed by depositing calcium carbonate weakens the corrosion tendency. The anodic Tafel slope (b_a) decreases slowly, and TH plays a certain

role in promoting this decrease. The cathodic Tafel slope (b_c) increases slightly, and TH has a certain inhibitory effect on this process.

3.6 Correlation analysis

A correlation analysis of the above experimental results was carried out to determine the sensitivity of various factors to the corrosion rate. Table 18 shows the correlation analysis results for the internal corrosion influencing factors.

Table 18. Correlation analysis of internal corrosion influencing factors

Influencing factor	T	pH	DO	TRC	TH	Corrosion rate
T	1.000					
pH	-0.678	1.000				
DO	0.121	-0.180	1.000			
TRC	-0.244	0.299	-0.037	1.000		
TH	0.105	0.055	-0.254	0.054	1.000	
Corrosion rate	0.498	-0.469	0.338	-0.007	-0.318	1.000

From Table 18, it can be seen that temperature and DO are positively correlated with the corrosion rate and that the corrosion rate is negatively correlated with pH and TH, while TRC is almost irrelevant to the corrosion rate. Comparing the correlation coefficient (r) of each influencing factor and the corrosion rate, it is found that the order of the effect of the factors on the corrosion rate is temperature > pH > DO > TH > TRC.

Then, the correlation between the influencing factors was analysed, and the results are as follows. (1) There is a significant negative correlation between temperature and pH ($r = -0.678$). In addition to accelerating the rates of the cathodic and anodic reactions, a temperature increase can also reduce the pH and further increase the corrosion rate. (2) There is a positive correlation between pH and TRC ($r = 0.299$), which is mainly due to the use of sodium hypochlorite as a TRC concentration-modulating reagent in the experiment. It is a weak acid salt and causes a slight increase in pH by hydrolysis. Due to the lower TRC concentration in the experimental conditions, the effect on the corrosion rate is not significant. (3) There is a certain negative correlation between DO and TH ($r = -0.254$). This may be because the increase in the DO concentration is conducive to the formation of corrosion scales, which leads to the deposition of calcium and magnesium ions in the water, resulting in a lower TH. (4) The correlation between TH and pH was not significant ($r = 0.055$), indicating that TH mainly reduces the corrosion rate by depositing a protective layer on the surface of the corrosion scale rather than indirectly affecting the corrosion process by changing the pH.

4. CONCLUSIONS

Based on the FCSMS, the factors influencing the internal corrosion of ductile iron pipes were systematically studied using electrochemical testing techniques. The conclusions are as follows.

Under the influence of five factors, the corrosion of ductile iron proceeds through three stages.

The corrosion rate increases with increasing temperature and shows a clear linear relationship. Increasing temperature is conducive to the growth of corrosion scale and accelerates the stability of scale. Increasing temperature can simultaneously promote the anodic and cathodic reactions.

The corrosion rate increases with increasing DO concentration. DO promotes the growth of scale, and a high concentration of DO is conducive to the stability of scale. DO participates in the corrosion reaction of ductile iron as the main cathode depolarizer.

The corrosion rate decreases linearly with increasing pH. The density of the corrosion scale is significantly enhanced at high pH. The increase in pH suppresses both the anodic and cathodic reactions but mainly suppresses the cathodic reaction.

The TRC concentration has little effect on the corrosion rate. A high concentration of TRC is not conducive to the stability of scale. TRC has no effect on the anodic reaction. The increase in TRC concentration promotes the cathodic reaction.

The corrosion rate decreases slightly with increasing TH. The increase in TH is beneficial to the stability of scale. TH can promote the anodic reaction and inhibit the cathodic reaction.

The order of the influence of various factors on the corrosion rate is temperature > pH > DO > TH > TRC.

ACKNOWLEDGEMENT

We are grateful for the support provided by the National Natural Science Foundation of China (No. 51278333).

References

1. F. Teng, Y. T. Guan and W. P. Zhu, *Corros. Sci.*, 50 (2008) 2816.
2. Y. Zhu, H. Wang, X. Li, C. Hu, M. Yang and J. Qu, *Water Res.*, 60 (2014) 174.
3. H. Wang, C. Hu, L. Zhang, X. Li, Y. Zhu and M. Yang, *Water Res.*, 65 (2014) 362.
4. Y. Zou, J. Wang and Y. Y. Zheng, *Corros. Sci.*, 53 (2011) 208.
5. R. de Levie, *Adv. Electrochem. Electrochem. Eng.*, 6 (1967) 329.
6. I. Frateur, C. Deslouis, M. E. Orazem and B. Tribollet, *Electrochim Acta*, 44 (1999) 4345.
7. O. E. Barciaa, E. D'Eliaa, I. Frateurb, O. R. Mattos, N. Pébère and B. Tribollet, *Electrochim Acta*, 47 (2002) 2109.
8. M. Sancy, Y. Gourbeyre, E. M. M. Sutter and B. Tribollet, *Corros. Sci.*, 52 (2010) 1222.
9. H. Y. Tong, P. Zhao, H. W. Zhang, Y. M. Tian, X. Chen, W. G. Zhao and M. Li, *Chemosphere*, 119 (2015) 1141.
10. L. S. Mcneill and M. Edwards, *Environ Monit Assess*, 77 (2002) 229.
11. R. W. Bonds, L. M. Barnard, A. M. Horton and G. L. Oliver, *J Am Water Works Ass*, 97 (2005) 88.
12. P. Sarin, V. L. Snoeyink, J. Bebee, K. K. Jim and M. A. Beckett, *Water Res.*, 38 (2004) 1259.
13. Z. Yan and M. Edwards, *J Water Supply Res T*, 56 (2007) 55.
14. S. Masters, H. Wang, A. Pruden and M. A. Edwards, *Water Res.*, 68 (2015) 140.
15. H. Wang, C. Hu, X. Hu, M. Yang and J. Qu, *Water Res.*, 46 (2012) 1070.
16. D. A. Lytle, T. L. Gerke and J. B. Maynard, *J Am Water Works Ass*, 97 (2005) 109.
17. H. Sun, B. Shi, D. A. Lytle, Y. Bai and D. Wang, *Environ Sci Proc Impacts*, 16 (2014) 576.
18. I. Frateur, C. Deslouis, M. E. Orazem and B. Tribollet, *Electrochim Acta*, 44 (1999) 4345.

19. O. E. Barcia, E. D'Elia, I. Frateur, O. R. Mattos, N. Pébère and B. Tribollet, *Electrochim Acta*, 47 (2002) 2109.
20. M. Sfaira, A. Srhiri, H. Takenouti, M. M. D. Ficquelmont-Loizos, A. B. Bachir and M. Khalakhil, *J Appl Electrochem.*, 31 (2001) 537.
21. M. Sancy, Y. Gourbeyre, E. M. M. Sutter and B. Tribollet, *Corros. Sci.*, 52 (2010) 1222.
22. J. F. Rios, J. A. Calderón and R. P. Nogueira, *Corrosion*, 69 (2013) 875.
23. H. Guo, Y. M. Tian, H. L. Shen, X. F. Liu and Y. Chen, *Int J Electrochem Sci.*, 11 (2016) 6993.
24. J. C. Rushing, Advancing the Understanding of Water Distribution System Corrosion: Effects of Chlorine and Aluminum on Copper Pitting, Temperature Gradients on Copper Corrosion, and Silica on Iron Release, Virginia Tech, (2002) Virginia, U.S.A.
25. X. H. Nie, X. G. Li, C. W. Du and Y. F. Cheng, *J Appl Electrochem.*, 39 (2009) 277.
26. Z. Tang, S. Hong, W. Xiao and J. Taylor, *Corros. Sci.*, 48 (2006) 322.
27. Z. L. Mi, X. J. Zhang and C. Chen, *Desalin Water Treat.*, 57 (2016) 9728.
28. H. Krawiec, V. Vignal and J. Banas, *Ecs Trans.*, 3 (2007) 623.
29. F. O. Aramide, E. O. Olorunniwo, P. O. Atanda and J. O. Borode, *J Miner Mater Charact Eng*, 9 (2010) 867.
30. J. Liang, A. Deng, R. J. Xie, M. Gomez, J. Y. Hu, J. F. Zhang, C. N. Ong and A. Adin, Corrosion kinetics of ductile iron in remineralized RO desalinated seawater, CORROSION 2013 Conference & Expo, Orlando, U.S.A, 2013, 2557.

© 2018 The Authors. Published by ESG (www.electrochemsci.org). This article is an open access article distributed under the terms and conditions of the Creative Commons Attribution license (<http://creativecommons.org/licenses/by/4.0/>).